Hindawi
Advances in Polymer Technology
Volume 2019, Article ID 8124351, 9 pages
https://doi.org/10.1155/2019/8124351

Research Article

Studying Ni(II) Adsorption of Magnetite/Graphene Oxide/Chitosan Nanocomposite

Luyen T. Tran,[1] Hoang V. Tran,[1] Thu D. Le,[1] Giang L. Bach,[2] and Lam D. Tran[3]

[1]*School of Chemical Engineering, Hanoi University of Science and Technology, 1 Dai Co Viet Road, Hanoi, Vietnam*
[2]*Nguyen Tat Thanh University, 300A Nguyen Tat Thanh, Ho Chi Minh City, Vietnam*
[3]*Institute for Tropical Technology, VAST, 18 Hoang Quoc Viet, Cau Giay, Hanoi, Vietnam*

Correspondence should be addressed to Thu D. Le; thu.ledieu@hust.edu.vn

Received 31 May 2019; Accepted 4 July 2019; Published 1 August 2019

Academic Editor: Gyorgy Szekely

In this paper, Fe_3O_4/graphene oxide/chitosan (FGC) nanocomposite was synthesized using coprecipitation method for application to removal of nickel ion (Ni(II)) from aqueous solution by adsorption process. To determine residue Ni(II) ions concentration in aqueous solution after adsorption process, we have used UV-Vis spectrophotometric method, which is an effective and exact method for Ni(II) monitoring at low level by using dimethylglyoxime (DMG) as a complex reagent with Ni(II), which has a specific adsorption peak at the wavelength of 550 nm on UV-Vis spectra. A number of factors that influence Ni(II) ions adsorption capacity of FGC nanocomposite such as contact time, adsorption temperature, and adsorbent dosage were investigated. Results showed that the adsorption equilibrium is established after 70 minutes with the adsorbent dosage of 0.01 $g.mL^{-1}$ at 30°C (the room temperature). The thermodynamic and kinetic parameters of this adsorption including free enthalpy change (ΔG^0), enthalpy change (ΔH^0), entropy change (ΔS^0), and reaction order with respect to Ni(II) ions were also determined. The Ni(II) ions adsorption equilibrium data are fitted well to the Langmuir isotherm and the maximum monolayer capacity (q_{max}) is 12.24 $mg.g^{-1}$. Moreover, the FGC adsorbent can be recovered by an external magnet; in addition, it can be regenerated. The reusability of FGC was tested and results showed that 83.08% of removal efficiency was obtained after 3 cycles. The synthesized FGC nanocomposite with many advantages is a promising material for removal of heavy metal ions from aqueous solution to clean up the environment.

1. Introduction

Nickel ion (Ni(II)) is mainly generated from petroleum procedure, plating industry wastewater which is released into the natural environment and is toxic to nature. Drinking of nickel(II) polluted water for a long time will cause cancer, lungs and nervous system problem, or dry cough [1]. Therefore, removal of Ni(II) from the aquatic environment is a serious environmental problem in view of public health. Graphene with high specific surface area, chemical stability, and excellent electrical, thermal properties [2] recently has received increasing attention of researchers all over the world in the area of adsorption. However, the disadvantages of graphene sheets are that, in the water environment, they are poorly soluble and tend to aggregate, which significantly reduces the surface area and adsorption capacity. Thus, graphene oxide (GO), the intermediate product of oxidation of graphite, with many oxygen-rich functional groups (epoxy, hydroxyl, and carbonyl groups), is an attractive object for many research areas such as detection of DNA [3], matrix composite membranes, or film [4–6], especially in removal of heavy metal ions and organic pollutants from aqueous solutions. In recent years, a number of reports have been published on the adsorption of heavy metal ions by using GO and GO-based materials as an adsorbent. Table 1 listed the maximum adsorption capacity of some heavy metal ions on GO and some GO-based materials. From that, GO proves the strong adsorption affinity and is a good adsorption material.

In this study, we have synthesized Fe_3O_4/graphene oxide/chitosan (FGC) nanocomposite and used it as recoverable adsorbent for the adsorption of Ni(II) ions in aqueous solution with the ambition of using functional groups (epoxy, carboxyl) of graphene and amino, hydroxyl groups of chitosan to enhance the adsorption interactions with heavy

Table 1: Comparison of adsorption capacity of GO and GO-based materials for heavy metal ions removal.

Adsorbent	Applied to metal ions	q_{max} ($mg.g^{-1}$)	Working conditions	Reusability	Reference
GO	Co(II)	21.28	pH5.5; 298K	None	[7]
Magnetic Chitosan - GO (MC-GO)	Pb(II)	92%	pH5.0	78% after 4 cycles	[8]
Chitosan-GO	Cr(VI)	104	pH2.0	82% after 10 cycles	[9]
GO-Carbon Composite (GO - CC)	Pb(II)	68.8		None	[10]
GO	Cu(II)	277.77	pH6.0, ambient temperature	Reduced by 4.5% after 5 cycles	[11]
rGO	Pb(II) Cd(II) Cu(II) Mn(II)	413.22 162.33 55.34 42.46	298K	Decreased nearly by 20% after 3 cycles	[12]
GO	Cd(II)	86.2	pH 7, Room temperature	None	[13]
GO	Zn(II)	208.33	pH 7.0, 293K	Reduced nearly by 8% after 6 cycles	[14]
GOCC	Ni(II)	138.31	293K	None	[15]
GO	Ni(II)	38.61	298K, pH 6	None	[16]
Graphene nanosheet/MnO_2	Ni(II)	46.55	Room temperature	91% after 5 cycles	[17]

metal ions to reduce the high cost of graphene materials and increase the efficiency of the process. By using a magnetic material (Fe_3O_4), the separation of small particle size of adsorbent will be rapid and the secondary discharge to environment will be avoided. The different equilibrium conditions and kinetics of adsorption Ni(II) are also investigated in detail.

2. Experimental

2.1. Chemical and Reagents. Graphite was extracted from pencils which were purchased from a local bookstore. Dimethylglyoxime ($CH_3C(NOH)C(NOH)CH_3$) (DMG), sulfuric acid (H_2SO_4) 98 wt.%, sodium nitrate ($NaNO_3$), potassium permanganate ($KMnO_4$), $NiCl_2.6H_2O$, iron(III) chloride hexahydrate ($FeCl_3.6H_2O$), iron(II) sulfate heptahydrate ($FeSO_4.7H_2O$), chitosan (CS), acetic acid (CH_3COOH) solution 30 wt.%, and sodium hydroxide (NaOH) were purchased from Sigma Aldrich.

2.2. Preparation of Fe_3O_4/Graphene Oxide/Chitosan (FGC) Nanocomposite. Fe_3O_4/graphene oxide/chitosan (FGC) materials were synthesized using coprecipitation method as previously reported [18] with several modifications. Three precursors, $FeSO_4.4H_2O$, $FeCl_3.6H_2O$ solution with the molar ratio of 2:1; GO dispersion, and chitosan (2.5 wt.%) solution, are used directly without any purification. The composition of sample in this study is Fe_3O_4 : GO : CS = 42.5 : 7.5 : 50 (in mass), whereby a mixture of three precursors with various volumes was stirred continuously (using IKA magnetic stirrer with stirring rate of 200 rpm) in a flask for 30 minutes to obtain a homogeneous mixture. NaOH solution is dropped slowly to this flask to obtain the Fe_3O_4/GO/CS suspension. This suspension was kept at room temperature for 18 hours without stirring and then washed by distilled water for many times to remove all base (pH reaches 7). It was dried in vacuum at 78°C for 18 hours; we obtained the FGC adsorbent. XRD pattern and transmission electron microscopy (TEM) of GO, Fe_3O_4, and FGC adsorbent are shown in Figure SI.1 and Figure SI.2 in supporting information (SI), respectively.

2.3. Batch Experiments. A stock of Ni(II) solution is prepared by dissolving $NiCl_2.6H_2O$ in distilled water (5.8 $g.L^{-1}$). Experimental solutions with different concentrations are obtained by diluting a stock solution. A typical adsorption experiment was carried out through the following procedure: 10 mg of FGC powder was added to 1 mL of Ni(II) containing solution. This mixture was stirred for adsorption process in a water batch for 70 minutes. Then, FGC nanocomposite was removed by an external magnet and residue Ni(II) in solution will be determined.

2.4. Methodology. Working solutions were prepared daily, consisting of 1.725 mL distilled water, 0.1 mL DMG solution, 0.3 mL ammonia solution, 0.25 mL saturated Br_2 solution, and 0.125 mL experimental solution. The intensity of color was measured using UV-Vis spectrophotometer. The effects of contact time, temperature, and kinetics of Ni(II) adsorption on FGC nanocomposite were studied. After that, the adsorbent was regenerated to see the reusability of this material.

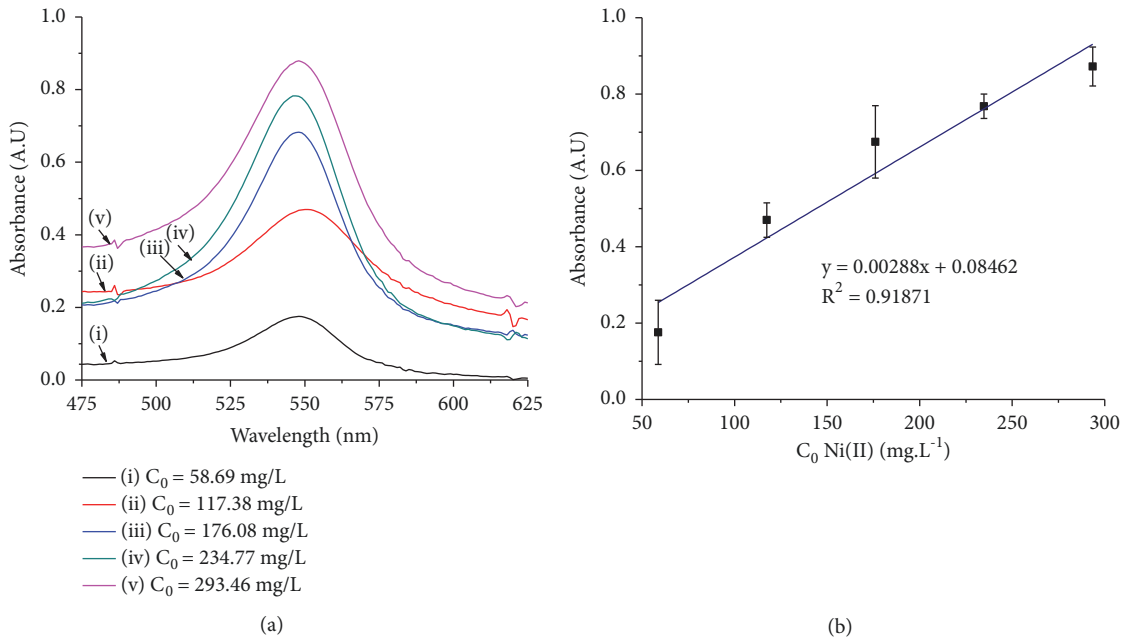

(a) (b)

FIGURE 1: (a) UV-Vis spectra of Ni(II) solutions with different concentrations; (b) the calibration curve for Ni(II) concentration determination.

The reaction order with respect to Ni(II) ions was studied using Lambert-Beer equation as described in

$$A = \varepsilon(\lambda).l.C \tag{1}$$

where A is absorbance, $\varepsilon(\lambda)$ is a molar absorbed factor (this factor changes by changing λ and it characterizes each substance), l is a length of cuvette, and C is concentration of Ni(II) solution vs. time. Thus, if absorbance of a substance is measured at a known wavelength (λ) and l = 1 cm constant, so absorbance (A) only depends on concentration (C). Therefore, to estimate the reaction order with respect to Ni(II) ions, the relation between absorbance A and time t is investigated, instead of investigating the relation between C and time t, using the following Eq.:

$$\ln\frac{C_t}{C_0} = \ln\frac{(A - A_e)}{(A_0 - A_e)} \tag{2}$$

where A_0 and A_e are the initial and equilibrium absorbance, respectively; A is the absorbance at time t; C_0 and C_t are the initial concentration and the concentration at time t, respectively. Thus, the reaction order with respect to Ni(II) ions is extracted by drawing the plot of ln(A-A_e) vs. t.

The amount of Ni(II) ions uptake by FGC (q_e, mg.g^{-1}) was calculated by the following equation:

$$q_e = \frac{C_0 - C_e}{m_a} \tag{3}$$

where C_0 and C_e (mg.L^{-1}) are the initial and equilibrium concentrations of Ni(II) ions in solution, respectively; m_a is the concentration of FGC (g.L^{-1}).

The thermodynamic parameters of the Ni(II) ions adsorption such as enthalpy change (ΔH^0), entropy change (ΔS^0), and free enthalpy change (ΔG^0) are also calculated using the following equations [16]:

$$K^0 = \frac{C_0 - C_e}{C_e} \tag{4}$$

$$\Delta G^0 = -RT\ln K^0 \tag{5}$$

$$\Delta G^0 = \Delta H^0 - T\Delta S^0 \tag{6}$$

$$\ln K^0 = \frac{\Delta S^0}{R} - \frac{\Delta H^0}{RT} \tag{7}$$

where C_0 and C_e are the initial and equilibrium concentrations of Ni(II) ions (mol.L^{-1}), respectively; R is gas constant (R = 8,314 J.mol^{-1}.K^{-1}); T is absolute temperature (K).

The Langmuir equation is given as in the following Eq.:

$$\frac{C_e}{q_e} = \frac{1}{K_L.q_{max}} + \frac{1}{q_{max}}.C_e \tag{8}$$

where q_e (mg.g^{-1}) is the amount of Ni ions adsorbed at equilibrium, q_{max} (mg.g^{-1}) is the maximum Ni ions adsorption amount, and K_L is the equilibrium adsorption constant.

The Freundlich isotherm is given as:

$$\log q_e = \log K_F + \frac{1}{n}\log C_e \tag{9}$$

where K_F and n are Freundlich constant and obtained from the intercept and the slope of the linear plot of log q_e vs. log C_e.

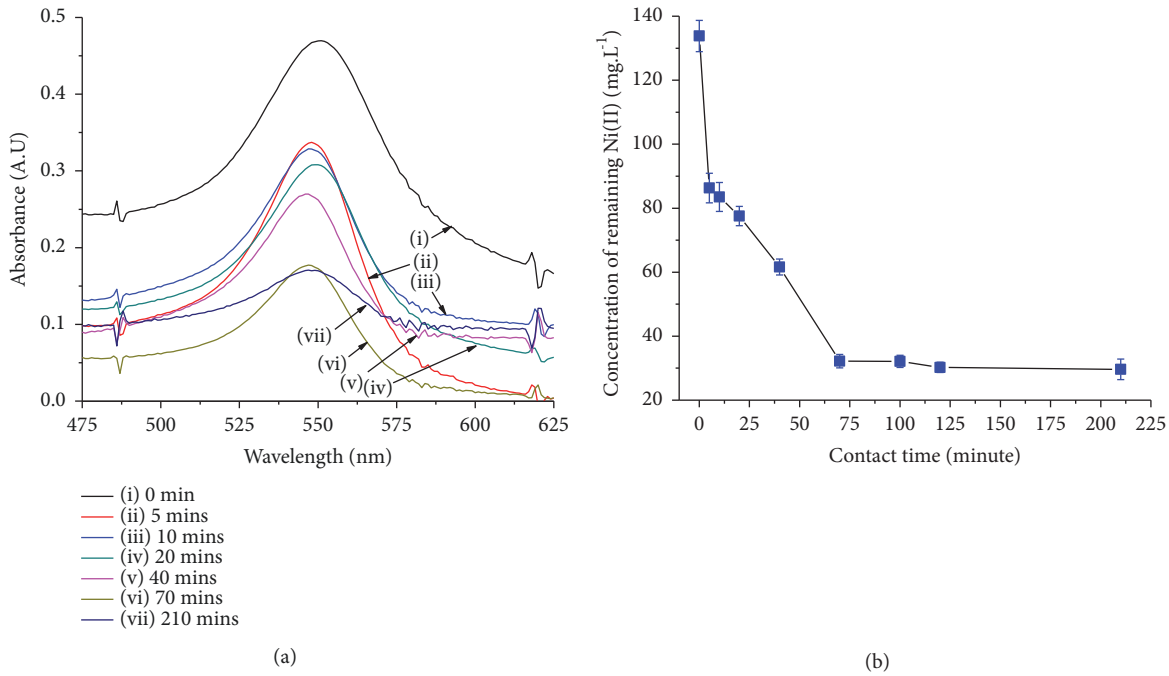

FIGURE 2: (a) UV-Vis spectra of Ni(II) solution after adsorption process; (b) effect of contact time on concentration of remaining Ni(II) ions. Experiment conditions: C_0 = 135 mg.L^{-1}; T = 30°C.

3. Results and Discussion

3.1. Calibration Curve. DMG was used to recognize the small amount of Ni(II) in the solution by spectroscopy. In the presence of Ni(II) ion, the solution containing DMG color will change from colorless to red color. The red color is darker if the Ni ion content is high. 1.2% alcoholic DMG solutions were obtained by dissolving the amounts of the solid in absolute ethanol and used within no more than 2 weeks. To generate a calibration curve for determination Ni(II) residue in solution, various solutions with different Ni(II) concentrations in DMG were prepared. Ni(II) ions in aqueous solution with low concentration values were determined effectively and exactly by UV-Vis spectrophotometric method using DMG as a complex reagent at wavelength of 550 nm. Figure 1(a) shows UV-Vis spectra of Ni(II) solutions with different Ni(II) concentrations. Figure 1(b) shows the calibration curve for determining of Ni(II) concentration in solution that has been generated by drawing the optical density at wavelength of 550 nm (OD_{550nm}) vs. Ni(II) concentration. The remaining concentrations of Ni(II) in solutions after adsorption process have been determined by measuring UV-Vis spectra and using the calibration curve (Figure 1(b)).

3.2. Effect of Contact Time. The UV-Vis spectra of 135 mg.L^{-1} Ni (II) solution after adsorption process are shown in Figure 2(a). From these experimental results, the concentration of remaining Ni(II) ions in the solution has been determined by using the calibration curve, Figure 1(b). The effect of contact time on the Ni(II) ions adsorption capacity is shown in Figure 2(b). The result indicates that, from 5 to 70 minutes, the concentration of the remaining Ni(II) ions in the solution decreases, so the adsorption capacity increases with the increasing contact time. In the first 70 minutes, the Ni(II) ions are adsorbed rapidly. The adsorption equilibrium is established after 70 minutes.

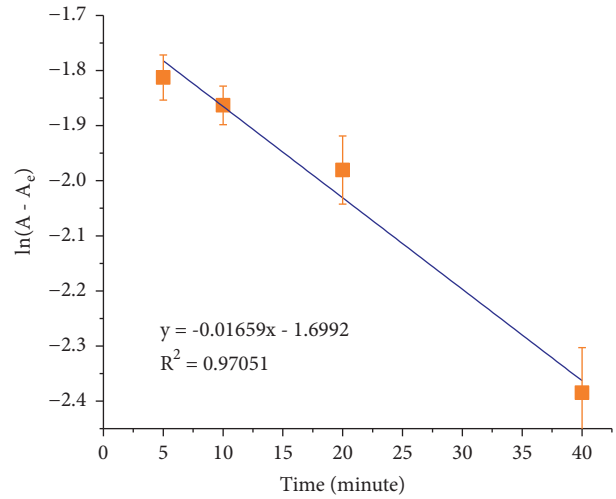

FIGURE 3: Plot of ln(A-A_e) vs. contact time (t) for determination of the reaction order with respect to Ni(II) ions. Experiment conditions: C_0 = 135 mg.L^{-1}; T = 30°C.

Using (1) and (2), the reaction order with respect to Ni(II) ions is extracted by drawing the plot of ln(A-A_e) vs. t, Figure 3. As can be seen in Figure 3, the obtained plot is nearly linear with the correlation coefficient (R^2 = 0.9705), which means the reaction order with respect to Ni(II) is 1 (the first order).

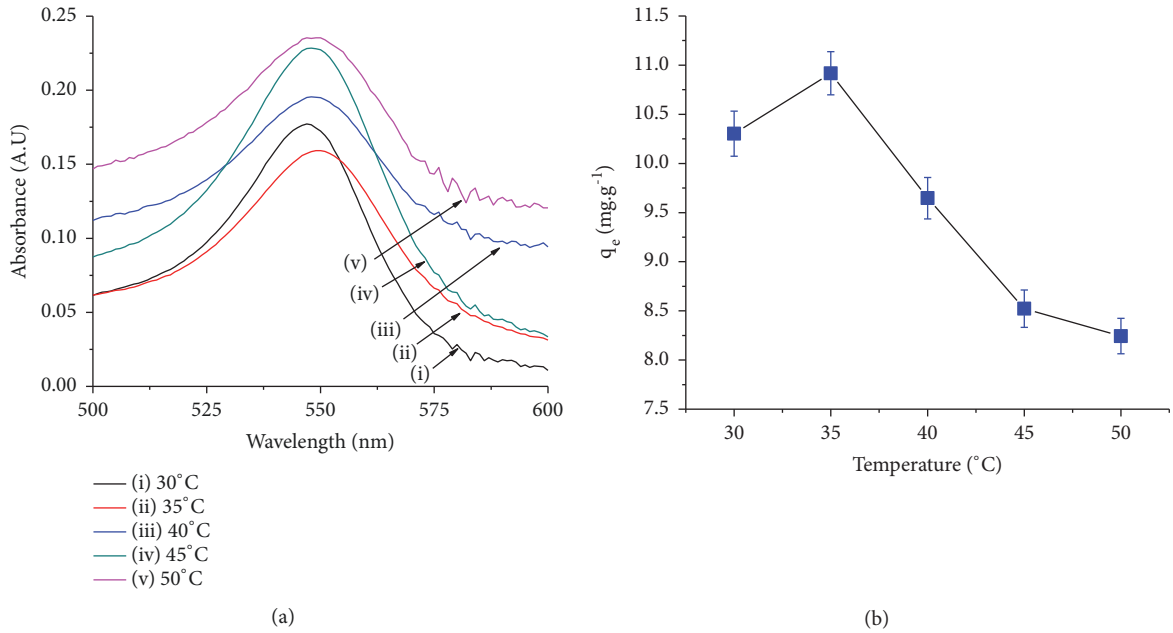

Figure 4: Effect of temperature on the Ni(II) ions adsorption on FGC nanocomposite. Experiment conditions: C_0 = 135 mg.L^{-1}; T = 30°C; 35°C; 40°C; 45°C; 50°C; contact time: 70 minutes.

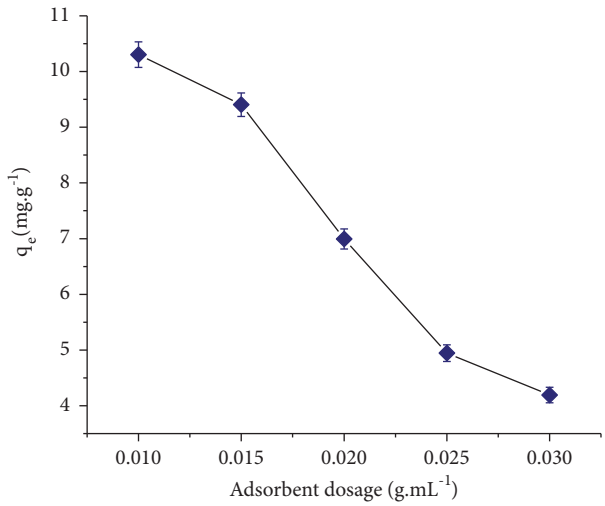

Figure 5: Effect of adsorbent dosage on the Ni(II) ions adsorption on FGC nanocomposite. Experiment conditions: C_0 = 135 mg.L^{-1}; T = 30°C; contact time: 70 minutes.

3.3. Effect of Temperature. The UV-Vis spectra of 135 mg.L^{-1} Ni (II) solutions after 70 minutes of adsorption process at different temperatures are shown in Figure 4(a). From these experimental results, the concentration of the remaining Ni(II) ions in the solution has been calculated by using the calibration curve, Figure 1(b). Then the amount of Ni(II) ions uptake by FGC (q_e, mg.g^{-1}) was calculated by using (3).

The effect of temperature on the Ni(II) ions adsorption capacity is shown in Figure 4(b). It can be seen in Figure 4(b) that the adsorption capacity increases with the increasing temperature from 30°C to 35°C. When the temperature continues to increase from 35°C to 50°C, the adsorption capacity decreases. This result can be attributed to the fact that at the high temperature and the pore sites of chitosan on the adsorbent surface are miniature and inactivated.

The values of ΔG^0 calculated by using (4), (5), and (6) at 303, 308, 313, 318, and 323 K are -2.95, -3.69, -2.39, -1.42, and -1.21 (kJ.mol^{-1}), respectively. The negative values of ΔG^0 indicate that the adsorption Ni(II) ions process is spontaneous. From the linear fit of lnK^0 vs. 1/T (see (7)), ΔH^0 and ΔS^0 values calculated are -30.97 kJ.mol^{-1} and -92.2 J.mol^{-1}.K^{-1}, respectively. The negative value of ΔH^0 indicates that the Ni(II) ions adsorption process is exothermic. The negative value of ΔS^0 shows the decreasing of randomness during the adsorption process of Ni(II) ions onto FGC surface.

3.4. Effect of Adsorbent Dosage. The effect of adsorbent dosage on the Ni(II) ions adsorption capacity of FGC nanocomposite is shown in Figure 5. The amount of FGC nanocomposite has been changed from 0.01 to 0.03 g.mL^{-1} in order to optimize the adsorbent dosage condition. As can be seen in Figure 5, the optimized amount of the adsorbent (FGC nanocomposite) is 0.01 g.mL^{-1}. With adsorbent dosage of 0.01 g.mL^{-1}, the Ni(II) ions adsorption capacity on FGC nanocomposite reaches the highest value (q_e = 10.30 mg.g^{-1}). This result indicates that the adsorbent has a high adsorption capacity, resulting in a small amount of adsorbent being able to adsorb maximum amount of Ni(II) ions in the solution.

3.5. Adsorption Isotherm. Langmuir and Freundlich adsorption isotherms (see (8) and (9)), respectively, were used to analyze the adsorption data. The Langmuir isotherm is

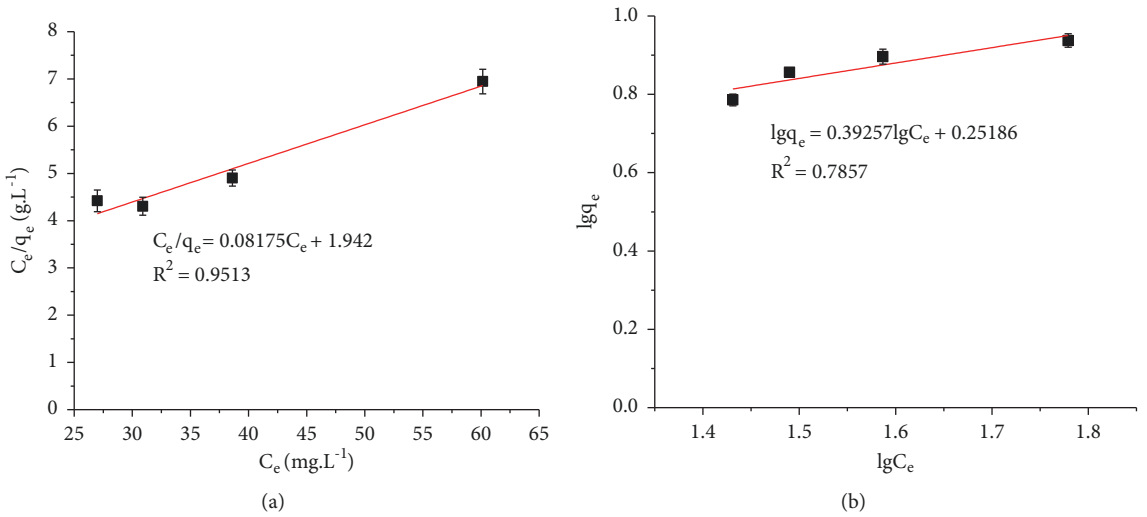

FIGURE 6: (a) Langmuir plot and (b) Freundlich plot.

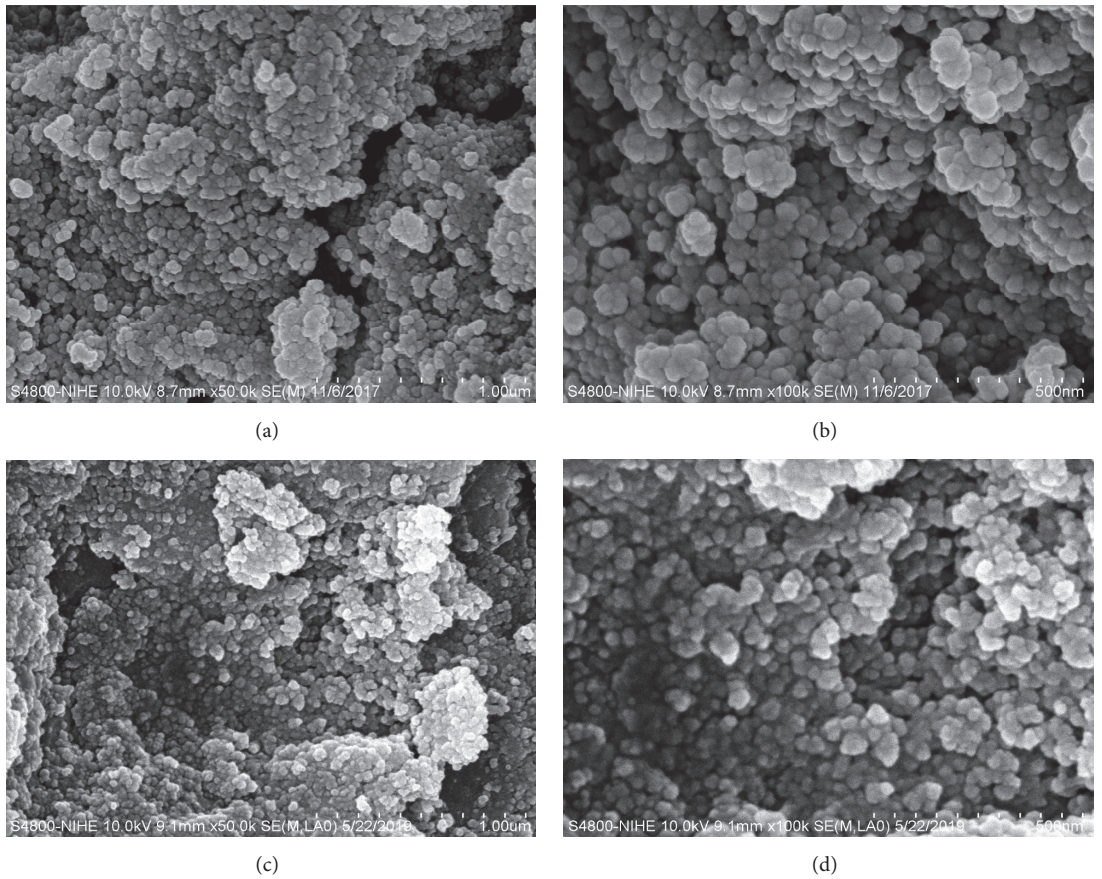

FIGURE 7: FESEM of FGC nanocomposite: (a, b) before and (c, d) after Ni(II) ions adsorption, respectively.

assumed for monolayer and homogeneous site of adsorbent surface without transmigration in the plane and uniform adsorption [19]. The Freundlich isotherm is valid for heterogeneous surface. The results are shown on Figure 6. Langmuir model with a higher correlation coefficient (R^2 = 0.9513) compares to R^2 of Freundlich (R^2 = 0.7857), indicating that the adsorption was fitted well to the Langmuir isotherm.

The maximum capacity q_{max} is 12.24 mg.g^{-1}; K_F and n are 1.79 and 2.55, respectively. With this value of n, the adsorption is favored [20] and the adsorption process is physical (n > 1)

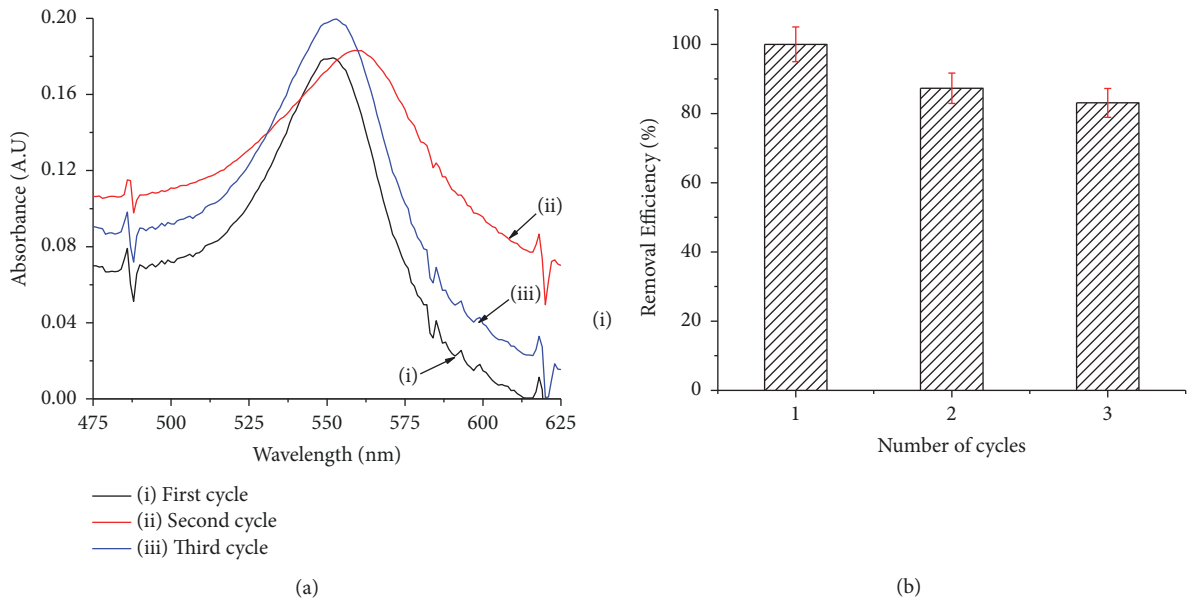

FIGURE 8: (a) UV-Vis spectra of Ni(II) solution after adsorption process using regenerated adsorbent; (b) Ni(II) removal efficiency of regenerated adsorbent. Experiment conditions: C_0 = 135 mg.L^{-1}; T = 30°C; contact time: 70 minutes.

TABLE 2: Comparison of adsorption capacity of some adsorbents for Ni(II) ions removal.

Materials	q_{max} (mg.g^{-1})	Ref.
Clay	2.75 – 21.14	[22]
Poly[N-(4-[4-(aminophenyl) methylphenylmethacrylamide])	6.13	[23]
Oxidized multiwall carbon nanotubes (MWCNTs)	9.43 at 303K	[24]
Natural clinoptilolite	0.96 at 293K	[25]
CS1501 RS 1301	2.3 – 5.8 1.5 – 5.1	[26]
This work	12.24	

[21]. Compared to other adsorbents, the adsorption capacity of FGC is higher than some adsorbents as clay [15] and CS1501 [19] as shown in Table 2.

3.6. Regeneration Studies. FESEM images of FGC nanocomposite before and after Ni(II) ions adsorption process are shown in Figures 7(a), 7(b), 7(c), and 7(d), respectively. It can be seen that the surface morphologies of FGC before and after Ni(II) ions adsorption are not changed. However, on FGC surface after Ni(II) adsorption (Figures 7(c) and 7(d)), the surface is coated by a layer of small particles with different contrast (Figures 7(a) and 7(b)), which can be attributed to uptake of Ni(II) onto FGC surface.

After recovery by an external magnet, FGC nanocomposite was regenerated by 0.1 M NaOH solution in 3 hours for deadsorption of Ni(II) ions. Then the adsorbent was cleaned many times with distilled water and dried for reuse.

The Ni(II) ions efficient removal of regenerated materials was compared to the original materials (as synthesized) and the results are shown in Figure 8. Figure 8(a) shows UV-Vis spectra of Ni(II) solutions before and after 1 to 3 adsorption-regeneration cycles. As can be seen in Figure 8(b), the Ni(II) ions efficient removal of FGC nanocomposite was still 83.08% after 3 adsorption-regeneration cycles. The adsorption capacity for Ni(II) ions slightly decreased; that is probably a result of losing binding sites after each desorption step [27]. In our future works, optimizing the pH of the solution used for deadsorption is really necessary in order to increase the Ni(II) ions adsorption capacity after a large number of adsorption-regeneration cycles. However, the above result has indicated that the synthesized FGC nanocomposite has a long-term stability and is fit for treating the heavy metal ions. In fact, in our previous work on adsorption Cr (VI) from aqueous solution, with the same material (FGC), q_{max} can reach 200 mg.g^{-1} at 298 K, pH 3 [28]. Therefore, this synthesized material can be used as a promising adsorbent for removal of heavy metal ions from aqueous solution.

4. Conclusion

This study indicated that Ni(II) ions can be removed from aqueous solution using synthesized FGC nanocomposite by adsorption method. Ni(II) ions in aqueous solution with lower concentration than 58.69 mg.L^{-1} were determined effectively and exactly by UV-Vis spectrophotometric method using dimethylglyoxime (DMG) as a complex reagent. The results show that the optimized adsorbent dosage for adsorption is 10 mg.mL^{-1} FGC with the Ni(II) ions initial concentration of 135 mg.L^{-1}. The thermodynamic parameters indicate that the adsorption process is spontaneous and exothermic and decreases the randomness. The adsorption fitted the Langmuir model well and the highest adsorption capacity is 12.24 mg.g^{-1}. After 3 cycles, the Ni(II) ions adsorption

capacity of FGC was about 83.08% comparing to the original sample, proving that it is a good material for removal of heavy metal ions in aqueous solution.

Data Availability

The data used to support the findings of this study are included within the article and included within the supplementary information file(s).

Conflicts of Interest

The authors declare that they have no conflicts of interest.

Supplementary Materials

XRD pattern and transmission electron microscopy (TEM) of GO, Fe3O4, and FGC adsorbent are shown in Figure SI.1 and Figure SI.2 in supporting information (SI), respectively. *(Supplementary Materials)*

References

[1] N. Jaafarzadeh, N. Mengelizadeh, M. Jalil, A. Takdastan, N. Alavi, and N. Niknam, "Removal of zinc and nickel from aqueous solution by chitosan and polyaluminum chloride," *International Journal of Environmental Health Engineering*, vol. 5, no. 1, p. 16, 2016.

[2] C. N. R. Rao, A. K. Sood, K. S. Subrahmanyam, and A. Govindaraj, "Graphene: the new two-dimensional nanomaterial," *Angewandte Chemie International Edition*, vol. 48, no. 42, pp. 7752–7777, 2009.

[3] B. Tian, Y. Han, J. Fock, M. Strömberg, K. Leifer, and M. F. Hansen, "Self-assembled magnetic nanoparticle–graphene oxide nanotag for optomagnetic detection of DNA," *ACS Applied Nano Materials*, vol. 2, no. 3, pp. 1683–1690, 2019.

[4] F. Fei, L. Cseri, G. Szekely, and C. F. Blanford, "Robust covalently cross-linked polybenzimidazole/graphene oxide membranes for high-flux organic solvent nanofiltration," *ACS Applied Materials & Interfaces*, vol. 10, no. 18, pp. 16140–16147, 2018.

[5] L. Cseri, J. Baugh, A. Alabi et al., "Graphene oxide–polybenzimidazolium nanocomposite anion exchange membranes for electrodialysis," *Journal of Materials Chemistry A*, vol. 6, no. 48, pp. 24728–24739, 2018.

[6] Z. Chen, F. Tong, D. Zhu, X. Lu, and Q. Lu, "Ductile polyimide/reduced graphene oxide nanohybrid films with porous structure fabricated by a green hydrogel strategy," *ACS Applied Polymer Materials*, vol. 1, no. 4, pp. 914–923, 2019.

[7] L. P. Lingamdinne, J. R. Koduru, H. Roh, Y. Choi, Y. Chang, and J. Yang, "Adsorption removal of Co(II) from waste-water using graphene oxide," *Hydrometallurgy*, vol. 165, pp. 90–96, 2016.

[8] M. S. Samuel, S. S. Shah, J. Bhattacharya, K. Subramaniam, and N. Pradeep Singh, "Adsorption of Pb(II) from aqueous solution using a magnetic chitosan/graphene oxide composite and its toxicity studies," *International Journal of Biological Macromolecules*, vol. 115, pp. 1142–1150, 2018.

[9] M. S. Samuel, J. Bhattacharya, S. Raj, N. Santhanam, H. Singh, and N. Pradeep Singh, "Efficient removal of Chromium(VI) from aqueous solution using chitosan grafted graphene oxide (CS-GO) nanocomposite," *International Journal of Biological Macromolecules*, vol. 121, pp. 285–292, 2019.

[10] T. Esfandiyari, N. Nasirizadeh, M. Dehghani, and M. H. Ehrampoosh, "Graphene oxide based carbon composite as adsorbent for Hg removal: Preparation, characterization, kinetics and isotherm studies," *Chinese Journal of Chemical Engineering*, vol. 25, no. 9, pp. 1170–1175, 2017.

[11] R. L. White, C. M. White, H. Turgut, A. Massoud, and Z. R. Tian, "Comparative studies on copper adsorption by graphene oxide and functionalized graphene oxide nanoparticles," *Journal of the Taiwan Institute of Chemical Engineers*, vol. 85, pp. 18–28, 2018.

[12] B. Wang, F. Zhang, S. He, F. Huang, and Z. Peng, "Adsorption behaviour of reduced graphene oxide for removal of heavy metal ions," *Asian Journal of Chemistry*, vol. 26, no. 15, pp. 4901–4906, 2014.

[13] N. Yari Moghaddam, B. Lorestani, M. Cheraghi, and S. Jamehbozorgi, "Adsorption of Cd and Ni from water by graphene oxide and graphene oxide-almond shell composite," *Water Environment Research*, vol. 91, no. 6, pp. 475–482, 2019.

[14] M. Pan, G. Wu, C. Liu, X. Lin, and X. Huang, "Enhanced adsorption of Zn(II) onto graphene oxides investigated using batch and modeling techniques," *Nanomaterials*, vol. 8, no. 10, p. 806, 2018.

[15] Y. Wu, H. Luo, H. Wang, L. Zhang, P. Liu, and L. Feng, "Fast adsorption of nickel ions by porous graphene oxide/sawdust composite and reuse for phenol degradation from aqueous solutions," *Journal of Colloid and Interface Science*, vol. 436, pp. 90–98, 2014.

[16] F. Najafi, O. Moradi, M. Rajabi et al., "Thermodynamics of the adsorption of nickel ions from aqueous phase using graphene oxide and glycine functionalized graphene oxide," *Journal of Molecular Liquids*, vol. 208, pp. 106–113, 2015.

[17] Y. Ren, N. Yan, Q. Wen et al., "Graphene/δ-MnO2 composite as adsorbent for the removal of nickel ions from wastewater," *Chemical Engineering Journal*, vol. 175, pp. 1–7, 2011.

[18] H. V. Tran, L. T. Bui, T. T. Dinh, D. H. Le, C. D. Huynh, and A. X. Trinh, "Graphene oxide/Fe3O4/chitosan nanocomposite: A recoverable and recyclable adsorbent for organic dyes removal. Application to methylene blue," *Materials Research Express*, vol. 4, no. 3, Article ID 035701, 2017.

[19] I. Langmuir, "The adsorption of gases on plane surfaces of glass, mica and platinum," *Journal of the American Chemical Society*, vol. 40, no. 9, pp. 1361–1403, 1918.

[20] L. Huang, Y. Sun, T. Yang, and L. Li, "Adsorption behavior of Ni (II) on lotus stalks derived active carbon by phosphoric acid activation," *Desalination*, vol. 268, no. 1-3, pp. 12–19, 2011.

[21] A. M. M. Vargas, A. L. Cazetta, A. C. Martins et al., "Kinetic and equilibrium studies: adsorption of food dyes Acid Yellow 6, Acid Yellow 23, and Acid Red 18 on activated carbon from flamboyant pods," *Chemical Engineering Journal*, vol. 181-182, pp. 243–250, 2012.

[22] S. S. Gupta and K. G. Bhattacharyya, "Adsorption of Ni(II) on clays," *Journal of Colloid and Interface Science*, vol. 295, no. 1, pp. 21–32, 2006.

[23] A. K. Kushwaha, N. Gupta, and M. Chattopadhyaya, "Dynamics of adsorption of Ni(II), Co(II) and Cu(II) from aqueous solution onto newly synthesized poly[N-(4-[4-(aminophenyl)methylphenylmethacrylamide])]," *Arabian Journal of Chemistry*, vol. 10, pp. S1645–S1653, 2017.

[24] C. Chen and X. Wang, "Adsorption of Ni(II) from aqueous solution using Oxidized multiwall carbon nanotubes," *Industrial &*

Engineering Chemistry Research, vol. 45, no. 26, pp. 9144–9149, 2006.

[25] A. Nezamzadeh-Ejhieh and M. Kabiri-Samani, "Effective removal of Ni(II) from aqueous solutions by modification of nano particles of clinoptilolite with dimethylglyoxime," *Journal of Hazardous Materials*, vol. 260, pp. 339–349, 2013.

[26] K. Kadirvelu, C. Faur-Brasquet, and P. L. Cloirec, "Removal of Cu(II), Pb(II), and Ni(II) by adsorption onto activated carbon cloths," *Langmuir*, vol. 16, no. 22, pp. 8404–8409, 2000.

[27] N. Zhang, H. Qiu, Y. Si, W. Wang, and J. Gao, "Fabrication of highly porous biodegradable monoliths strengthened by graphene oxide and their adsorption of metal ions," *Carbon*, vol. 49, no. 3, pp. 827–837, 2011.

[28] H. V. Tran, T. L. Tran, T. D. Le, T. D. Le, H. M. T. Nguyen, and L. T. Dang, "Graphene oxide enhanced adsorption capacity of chitosan/magnetite nanocomposite for Cr(VI) removal from aqueous solution," *Materials Research Express*, vol. 6, no. 2, Article ID 025018, 2019.